Annealing effect on the structural and electrical properties of LBMO thin films for uncooled bolometer applications

Ch. Seshendra Reddy[1,3*], A. Sivasankar Reddy[2], P. Sreedhara Reddy[3]
[1]*Department Material Science and Engineering, Shenzhen Graduate School, Harbin Institute Technology, University Town, Shenzhen 518055, China*
[2]*Department of physics, V.S.U. P.G. Centre, Kavali, Nellore-524001, India*
[3]*Department of Physics, Sri Venkateswara University, Tirupati–517502, India*

Abstract

$La_{0.7}Ba_{0.3}MnO_3$ (LBMO) thin films were deposited on silicon (Si (100))substrates by electron beam evaporation technique. The effect of post-annealing at different temperatures on the properties of structural, morphological and electrical was studied. All the films exhibited pseudocubic structure, with increasing annealing temperature from 873 K to 1173 K, the crystallization continuously takes place, together with oxidization process.When the annealing temperature increases the electrical resistivity of LBMO films gradually decreases due to the effect of increased crystallite size and mobility and a decrease in grain boundary density. Annealing temperature 1173 K, suggesting the LBMO films is suitable for bolometer applications.

Keywords: Thin films, bolometer, TCR, LBMO

* Corresponding Author: E-mail address:seshu123reddy@gmail.com (Ch. Seshendra Reddy)

1. Introduction

The uncooled bolometer is a device to measure the power of electromagnetic radiation and it is useful for the night vision, medical applications, and maintenance for plants, etc. The CMR (colossal magnetoresistance) materials has attracted a great deal of electronic phase separation,metal–insulator transition, [1–6], among spin, strong coupling, charge, orbital and have lattice degrees of freedom [7-8]and temperature dependence of the resistance (TCR), accompanied with considerably higher than that of the VOx film [9–14]. Goyal and co-workers studied the temperature of peak resistance (Tp) and TCR properties of different CMR materials, such as $La_{0.7}Ba_{0.3}MnO_3$(LBMO), $La_{0.7}Sr_{0.3}MnO_3$ (LSMO), $La_{0.7}Ca_{0.3}MnO_3$ (LCMO) and$Nd_{0.7}Sr_{0.3}MnO_3$ (NSMO), on different substrates with different conditions. In addition,

annealing has effectively improved the TCRof the perovskite manganese oxide film by PLD[10]. However, the temperature of the maximum TCR(Tm) was about 275 K whereas the TCR of the films was 4.0%.In this case, to improve the sensitivity of the IR sensor; it is necessary to cool the sensor. Lisauskas et al. reported that the TCRof the $La_{0.7}$ $(Pb_{0.63}Sr_{0.37})_{0.3}MnO_3$thin film was 7.4% at 295 K whereas the experimental temperature was very high[13]. In the present work, we choose single crystal Si substrates to prepare the LBMOfilms using electron beam evaporation for uncooled bolometer applications.The prepared films were annealed at different temperatures and characterized the films.

2. Experimental

Sample preparation and characterization

The LBMO target was prepared by using solid-state reaction method.High purity (99.99%) of La_2O_3, $BaCO_3$, and MnO_2 powders were mixed, grounded and calcinated at 873 K, the obtained single-phase powders were pelletized and annealed at 1373 K in air for 16 h. The deposition parameters of LBMO films shown Table 1. Before depositing the films, the Si substrate was cleaned with an ultrasonic cleaner and then rinsed in distilled water.

Parameters	Values
The target to substrate distance	50mm
Base pressure	1.33×10^{-5} Pa
Working pressure	2×10^{-4}Pa
Substrate temperature	773 K

Table1: Deposition parameters of LBMO thin films

Evaporation time	15 min
Accelerating voltage	5kV
Filament current	50mA
Annealing temperature	873, 1023 and 1173 K

The crystal structure of LBMO thin films was characterized by X-ray diffraction (XRD). The composition analysis of the films was analyzed by using energy dispersive spectroscopy (EDS). The morphology was observed by using atomic force microscopy (AFM). The electrical properties of the films were analyzed by using the standard four-probe method in the temperature range of 213 K to 333 K.

3. Results and discussions:

3.1 Structural properties

Fig.1 shows the XRD patterns of as-grown film and films annealed at various temperatures.Generally, annealing increases atomic mobility, enhancing the ability of atoms to find the most energetically favored sites; on the other hand, with the increase of the annealing temperature, the densities of the crystallographic defects including dislocations, interstitials in the LBMO thin films decreased. It was observed that all the films exhibited pseudocubic structure. All the films were annealed for 1 h. By increasing the annealing temperature from 873 to 1173 K, we noticed an increase of the (100), (110) and (200) peak intensities (Fig.1), indicating a probable improvement of the films crystallinity.

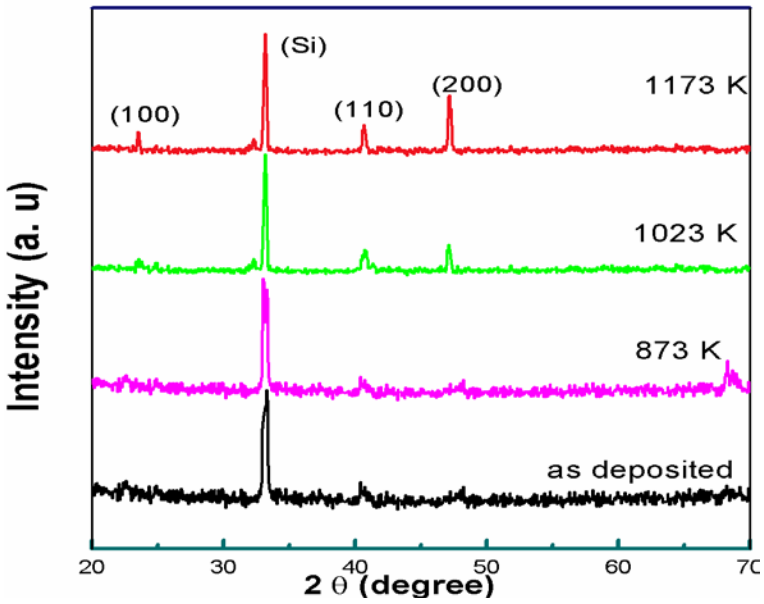

Fig.1: X-ray diffraction patterns of LBMO films annealed at different temperatures.

The 2θ shifts towards higher angle with increasing annealing temperature.It was found that, with increasing annealing temperature, the full-width at half-maximum (FWHM) became smaller, which is evidence for the improvement of the crystal quality. The XRDpatternof the film annealed at 873 K exhibited a low crystallinity which is probably due to an important amount of the amorphous phase.By increasing the annealing temperature, the amorphous film is being converted to an epitaxial phase of LBMO. The percentage of the amorphous phase could play an important role in the transport properties. The out-of-plane parameters can be determined from the symmetric XRD θ–2 θ scans.

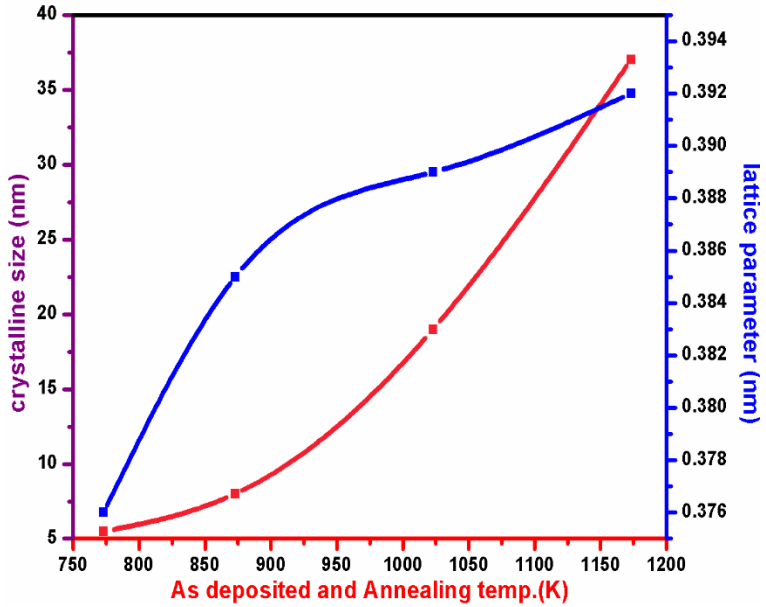

Fig.2: crystalline size and lattice parameter of the LBMO films annealed at different temperatures

The average crystallite size is increased with increasing annealing temperature revealing a fine nanocrystalline grain structure. Generally, the crystallite size depends on the annealing temperature [14].

The observed XRD data were indexed by matching with the data available for LBMO. Grain or cluster sizes were determined using the Scherrer formula.

$$d = \frac{k\lambda}{\beta Cos\,\Theta} \qquad (1)$$

β is the full width half maxima (FWHM) of the XRD peaks after subtracting, θ the Bragg angle, k is the practical factor (=0.91), $\lambda$is the wavelength of Cu Kα radiation.

Table 2: Crystalline size, lattice parameter values of LBMO thin films annealed at different temperatures.

Annealing temperature (K)	*Crystalline size (d) (nm)*	*Lattice parameter (a) (nm)*
773(as deposited)	*5.5*	*0.376*
873	*8*	*0.385*
1023	*19*	*0.389*
1173	*37*	*0.392*

The changes in the lattice parameter, grain size and stress of the LBMO films as a function of annealing temperature were given in Table 2. With increasing the annealing temperature from 873 to 1173 K, the grain size increases from 8 to 37 nm. This indicates an improvement in the crystalline nature of the film with an increase of annealing temperature. By increasing the annealing temperature from 873 to 1173 K, the calculated lattice parameter of the LBMO film increases slowly from 0.385 to 0.392 nm.Fig.2 shows the varying the crystalline size and lattice parameter with respect to the annealing temperature. The growth of granules with the increase of annealing temperature promotes the reduction of the number of non-bridging oxygen type defects favoring the formation of the LBMO grains.

3.2 Compositional analysis:

The composition of the as-grown films was analyzed by energy dispersive spectroscopy (EDS). The EDS spectra of the LBMO films annealed at different annealing temperatures were shown in Fig.3. From the figures, it was observed that the elements of La, Ba, Mn and O were observed in the LBMO films without any impurities. As-deposited and annealed films showed nearly stoichiometric ratio.

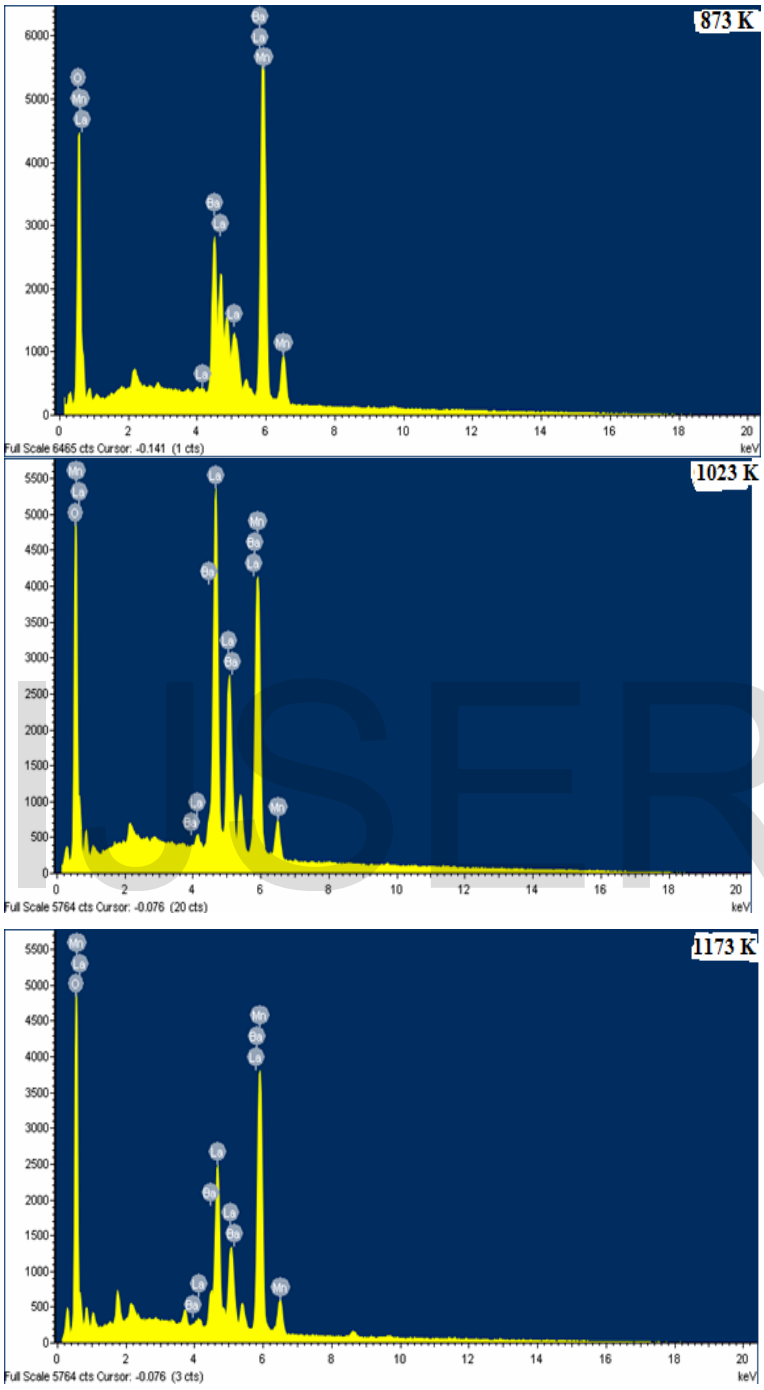

Fig.3: EDS patterns of the LBMO film annealed at different temperatures.

3.3 Surface morphology

The surface morphology of the films clearly altered with the annealing temperature. Fig.4 shows the surface morphology of LBMO thin films annealed at different temperatures (873, 1023 and

1173 K) on Si substrates. It is evident that different surface morphologies are developed gradually dependent on temperature during the annealing process.

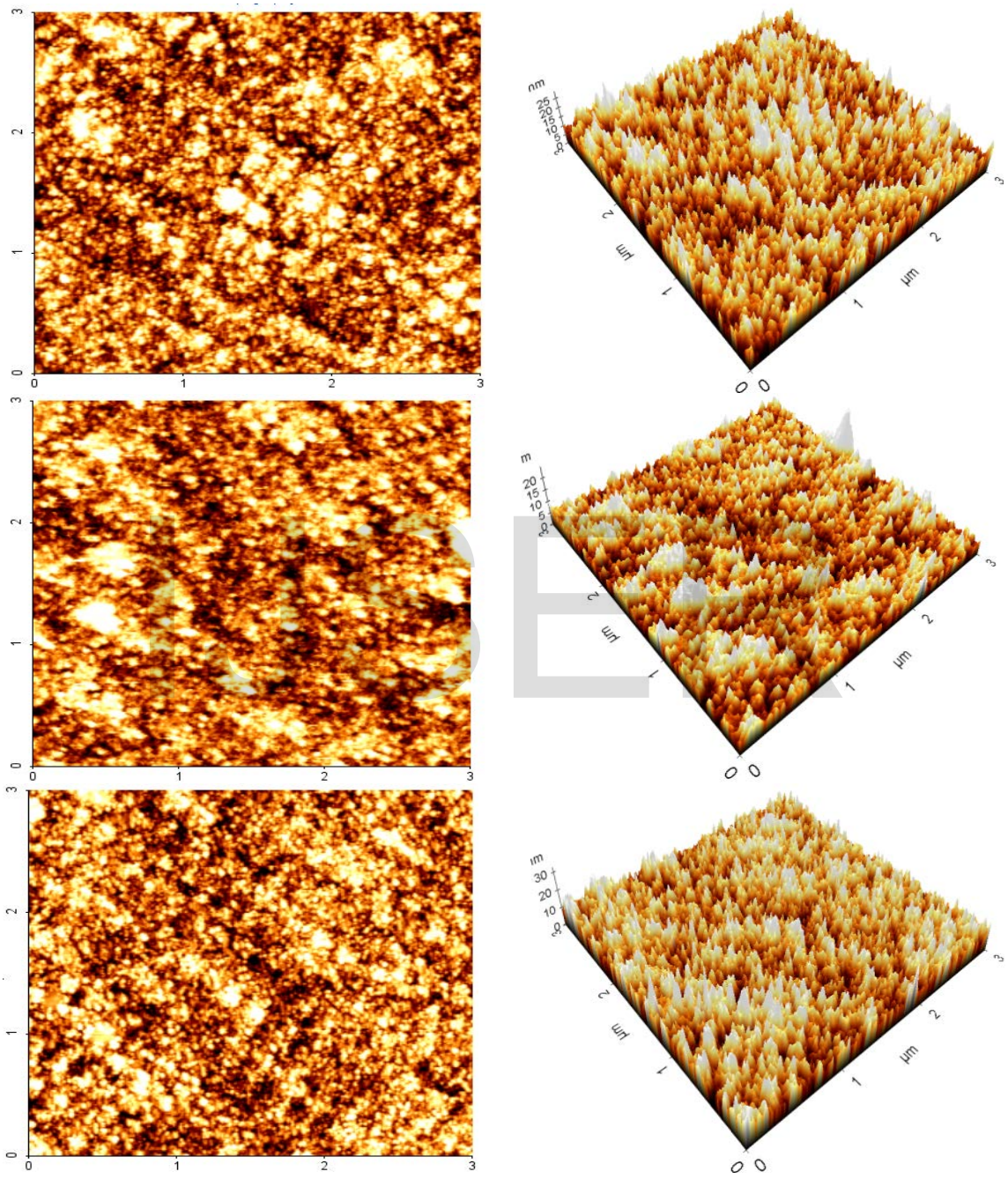

Fig.4: AFM images of LBMO films annealed at different temperatures (a) 873 (b)1023 and (c) 1173 K.

It was clearly seen that when the annealing temperature increases both the RMS roughness and grain size of the films also increased due to an increase in grain size. The grain boundaries

density is decreased and the large variation took place in grain growth on the films surface [15, 16]. From the AFM images, we can conclude that the quality of the thin film annealed at 1173 K was the highest.

3.4 Electrical properties

The electrical resistivity of LBMO thin films has a strong dependence on the microstructural defects and grain size. It was clear that the electrical properties of LBMO thin films were greatly affected by annealing temperature. The films showed a high electrical resistivity of 34.8 mΩ cm at annealing temperature 873 K. The electrical resistivity of the films decreased to 6.3 mΩ cm with increasing the annealing temperature to 1173 K. Fig.5 shows the temperature dependence of resistivity for the films annealed at different temperatures.

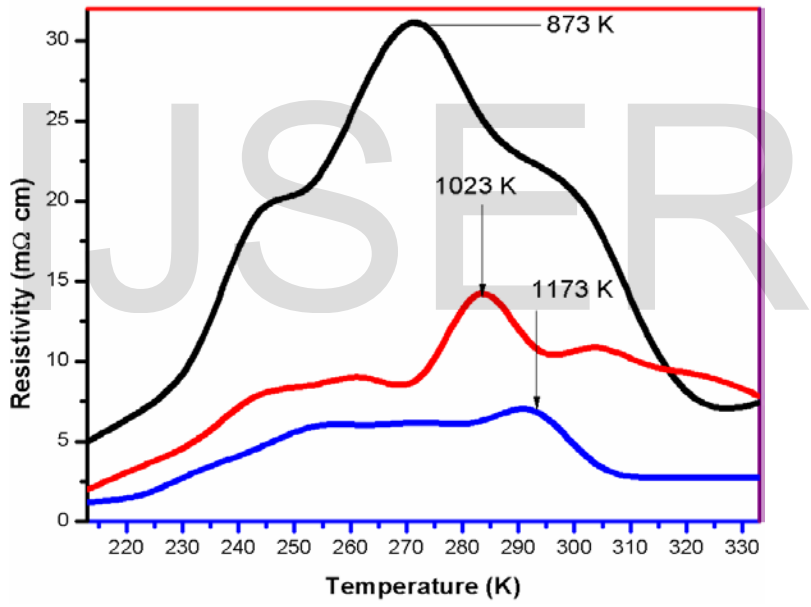

Fig.5: Variation of electrical resistivity of LBMO films annealed at different temperatures.

The films annealed at 1173 K shows the lower resistivity at the transition temperature (Tp). The increase of the transition temperature and the decrease in the resistivity under annealing is not surprising, since it is well known that microstructure and the electrical transport properties of the film can improve with heat treatment [17, 18], decrease in electrical resistivity was due to the increase in crystallite size, decrease in grain boundary density and increase the mobility of the films.

The temperature coefficient of resistance (TCR), which is the main factor of the electrical transport of CMR manganites, and it is calculated by TCR= (1/R*(dR/dT)*100)%. Getting the high TCR values at room temperature is the ultimate goal for the uncooled bolometric application. The temperature dependence of the TCR for films annealed at different temperatures is plotted in Fig.6. In the film annealed at 873 K, the TCR (TCRmax) is 3.5%/K at 260 K, and shifts to 5.14%/K at 295 K by increasing the annealing temperature to 1173 K and it is nearer to room temperature, higher TCR values were obtained at below room temperatures in CMR materials, such as $La_{0.67}Ca_{0.33}MnO_3$ (8% at 250 K) and $Nd_{0.7}Sr_{0.3}MnO_3$ (11% at 200 K) [15]. High Curie temperature with a low TCR value is achieved in $La_{0.67}Sr_{0.33}MnO_3$ (2% at 327 K) [13].

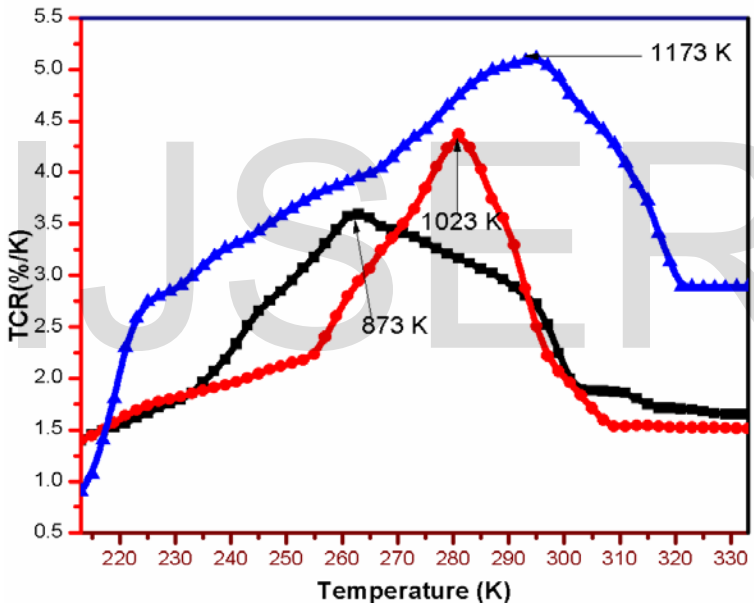

Fig.6: Variation of TCR of LBMO films annealed at different temperatures.

However, a higher TCR max value of 5.14% /K was observed at 296 K for the films annealed at high temperatures (1173 K), that means LBMO films useful for the uncooled bolometer applications.The obtained TCR value of the films annealed at 1173 K was higher than that of other bolometric materials such as amorphous silicon germanium alloys (SiGe, −1.8% /K), vanadium oxide (VOx,−1.7% /K) and $YBa_2Cu_3O_{7-x}$ superconducting materials (−3.2% /K) [19].

4.Conclusions:

Finally, the structure, composition, microstructure and electrical properties of deposited films were investigated in the annealing process. The study of annealing process shows LBMO thin film crystallize in a pseudocubic structure, with increasing annealing temperature, the crystallization continuously takes place, together with oxidization process.From surface morphology analysis it reveals that the annealing results in some increase in the crystal quality which describes that improvement in crystal structure properties of LBMO films and exhibits better electric properties with a TCR value of 5.14% /K near to the room temperature, which would be suitable for microbolometer. This work describes the one of the good technique to prepare uncooled bolometer LBMO materials by Electron beam evaporation with post annealing process.

References

[1] Ch. Renner, G. Aeppli, and H.M. Ronnow, "Charge ordering, stripes and phase separation in manganese perovskite oxides: An STM/STS study", Mater. Sci. Eng. C 25 (2005) 775.

[2] M. Uehara, S. Mori, C.H. Chen, and S.W. Cheong, "Percolative phase separation underlies colossal magnetoresistance in mixed-valentmanganites", Nature 399 (1999) 560.

[3] Ch. Renner, G. Aeppli, B.G. Kim, Y. Ah Soh, and S.W. Cheong, "Atomic-scale images of charge ordering in a mixed-valence manganite", Nature 416 (2002) 518.

[4] A. Antonakos, D. Lampakis, E. Liarokapis, M. Filippi, W. Prellier, G.H. Aydogdu, and H.U.Habermeier, "Phase separation in manganite thin films", J. Phys. Condens. Matter 20 (2008) 434232.

[5] N.H. Hong, J. Sakai, J.G. Noudem, A. Hassini, M. Gervais, and F. Gervais, "Ru-doped $La_{0.7}(Ba–Ca)_{0.3}MnO_3$ thin films: indirect evidence of phase separation", J. Phys. Condens.Matter 15 (2003) 6527.

[6] J.Zh. Wang, J.R. Sun, Q.Y. Dong, G.J. Liu, and B.G. Shen, "Magnetic relaxation and phase separation in manganite $Eu_{0.55}Sr_{0.45}MnO_3$", Solid State Commun. 149 (2009)325.

[7] C.H. Chen, and S.-W. Cheong, "Commensurate to Incommensurate Charge Ordering and Its Real-Space Images in $La_{0.5}Ca_{0.5}MnO_3$", Phys. Rev. Lett. 76 (1996) 4042.

[8] Z. Jirak, F. Damay, M. Hervieu, C. Martin, B. Raveau, G. Andreé, and F. Boureé, "Magnetism and charge ordering in $Pr_{0.5}Ca_xSr_{0.5-x}MnO_3$ (x=0.09 and 0.5)", Phys. Rev.B 61 (2000) 1181.

[9] M. Rajeswari, C.H. Chen, A. Goyal, C. Kwon, M.C. Robson, R. Ramesh, T. Venkatesan, and S. Lakeou, "Low-frequency optical response in epitaxial thin films of $La_{0.67}Ca_{0.33}MnO_3$ exhibiting colossal magnetoresistance", Appl. Phys. Lett. 68 (1996) 3555.

[10] A. Goyal, M. Rajeswari, R. Shreekala, S.E. Lofland, S.M. Bhagat, T.Boettcher, C. Kwon, R. Ramesh, and T. Venkatesan, "Material characteristics of perovskite manganese oxide thin

films for bolometric applications", Appl. Phys. Lett. 71 (1997) 2535.

[11] Ravi Bathe, K.P. Adhi, S.I. Patil, G. Marest, B. Hannoyer, and S.B. Ogale, "Silver ion implantation in epitaxial La2/3Ca1/3MnO*3* thin films: Large temperature coefficient of resistance for bolometric applications", Appl.Phys. Lett. 76 (2000) 2104.

[12] A. Lisauskas, S.I. Khartsev, and A. Grishin, "Tailoring the colossal magnetoresistivity: $La_{0.7}(Pb_{0.63}Sr_{0.37})_{0.3}MnO_3$ thin-film uncooled bolometer", Appl. Phys. Lett. 77 (2000) 756.

[13] J.H. Kim, S.I. Khartsev, and A. Grishin, "Epitaxial colossal magnetoresistance La0.67(Sr,Ca)0.33MnO3films on Si", Appl. Phys. Lett. 82 (2003) 4295.

[14] A.F. Khan, M. mehmood, A.M. Rana, and T. Muhammad, "Effect of annealing on structural, optical and electrical properties of nanostructured Ge thin films", App. Sur. Sci., 256 (2010) 2031.

[15] B. Ghosh, S. Kar, L.K. Bar, and A.K. Raychaudhuri, "Electronic transport in nanostructured films of $La_{0.67}Sr_{0.33}MnO_3$", J. Appl. Phys. 98 (2005) 094302.

[16] K.A. Thomas, P.S.I.P.N. De Silva, L.F. Cohen, A. Hossain, M. Rajeswari, T. Venkatesan, R. Hiskes, and J.L. MacManus-Driscoll, "Influence of strain and microstructure on magnetotransport in $La_{0.7}Ca_{0.3}MnO_3$ thin films", J. Appl. Phys. 84 (1998) 3939.

[17] W. Prellier, M. Rajeswari, T. Venkatesan, and R.L. Greene, "Effects of annealing and strain on thin films: A phase diagram in the ferromagnetic region", Appl. Phys. Lett. 75 (1999) 1446.

[18] D. Cao, F. Bridges, D.C. Worledge, C.H. Booth, and T. Geballe, "Effect of annealing temperature on local distortion of thin films", Phys. Rev. B 61 (2000) 11373.

[19] Lei Chang, Yijian Jiang, Lingfei Ji, "Effect of CO_2 laser irradiation on the transport properties of $La_{0.67}Ba_{0.33}MnO_3$ thin film", Solid State Communications, 141 (2007) 10, 582.